2021 43rd Annual International Conference of the
IEEE Engineering in Medicine & Biology Society (EMBC)
Oct 31 - Nov 4, 2021. Virtual Conference

Simulating Human Upper and Lower Limb Balance Recovery Responses Using Nonlinear Model Predictive Control

Keaton A. Inkol and John McPhee

Abstract— **The ability to generate predictive dynamic simulations of human movement using optimal control has been a growing point of interest in the design of medical/assistive devices, e.g. robotic exoskeletons. Despite this, many disseminated simulations of whole-body tasks, such as balance recovery, neglect the role of the upper body instead focusing on postural joints, e.g. ankle, knees, hips. Thus, the purpose of the current study was to use a novel nonlinear model predictive control (NMPC) approach to assess how actuated upper limbs, as well as different individual performance (optimality) criteria, can shape simulated reactive balance recovery responses. A sagittal biomechanical model of a young adult standing was designed and actuated via nonlinear muscle torque generators (rotational single-muscle equivalents). Forward dynamic simulations of balance recovery (NMPC-driven) following an *unexpected* support-surface perturbation were generated for each unique combination of selected performance criteria (6 total), perturbation direction (forward and backward), and arm joints free/locked. The observed joint trajectories provide insight into the emergence of human elements of postural control from individual optimality criteria, e.g. hip-ankle strategies emerge from single-joint regulation. Quantitative analysis of performance improvements with the arms free suggest that whether arm responses emerge in the simulations may be dependent on the problem's initial guess. Future work should focus on testing further performance criteria and improving NMPC as a model of the nervous system.**

I. INTRODUCTION

Recently, the U.S. Food and Drug Administration began encouraging engineers and researchers in health/medicine to implement computational modelling within the medical device design process [1]. Coincidentally, simulations of human musculoskeletal biomechanics have been gaining ground over the previous decades as a tool for investigating topics like injury risk and human motor control; this information can then be integrated into assistive device hardware and software, e.g. lower limb exoskeletons [6]. Typically, biomechanical simulations fall into one of two categories: inverse and forward dynamics. The latter is of noted interest as it facilitates construction of *what-if* scenarios, which can provide insight into device control robustness, human-device interactions, etc., without putting the end-user at risk.

Due to its implications in falls and injuries, balance control/recovery has been oft-used as the simulated movement of interest [4], [6], [7], [8], [11]. Most examples examine fixed-support strategies (e.g. ankle, hip strategy) [3] wherein the foot is considered a quasi-static body. To generate forward dynamic solutions, inputs to the biomechanical system must be known. Optimal control is often used to form inputs similar to the activations sent by the central nervous system (CNS). Ideally, human motor control models should feature concurrent feedforward and feedback elements [5]; however, many balance models reliant on feedback elements are limited in complexity [4], [6], [7], use a simple control scheme [11] or are driven by experimental tracking [12]. More complex musculoskeletal models [8], [9], [10] tend to rely on feedforward control, which inherently requires the perturbation delivered to the system to be a part of the dynamic model within the optimization. A good match between the dynamics of the control-oriented and system models implies that the responses to a truly novel perturbation cannot be captured; rather it is likely that the responses generated mimic those that occur after repeated exposure and habituation [8], [13]. Nonlinear model predictive control (NMPC) offers a novel solution to this problem [5]; it generates the inputs using constrained open-loop optimal control but operates with a receding horizon that subsequently closes the loop.

A common feature of many biomechanical simulations, not just balance, is the exclusion of arm motion, e.g. arms are rigidly fixed to trunk [6], [7], [8], [9], [12]. Those simulations that do include arms often have a particular component of the motor task that requires arms, e.g. pointing [5]. For a task like balance recovery, arm responses tend to be most overt following exposure to a novel and/or unexpected perturbation [13], and have quite a few hypothesized roles [14], [27]. Despite this, experimental protocols will often dictate that these segments are not to be used [8]. In the context of optimal control, this raises questions as to whether arm responses arise to reduce cost of movement according to some performance criteria. Answering this question would be beneficial for those designing predictive dynamic biomechanical simulations rooted in optimal control. Therefore, the current study used *what-if* simulations of balance recovery to assess whether arm strategies arise from a typical set of performance criteria following a novel balance perturbation. How these responses alter the actions at postural joints was also investigated. Key features of this approach included the investigation of multiple perturbation directions (in sagittal plane) and the use of NMPC as a model of the CNS.

II. MODEL, CONTROL, & SIMULATION

A. Human Biomechanical Model

The 5 degree-of-freedom (DOF) biomechanical model of upright stance, see Fig. 1, was designed in MapleSim (Maplesoft, Canada). Bilateral ankle, knee, hip, shoulder,

*This work was supported by the Canada Research Chairs Program and the Natural Sciences and Engineering Research Council of Canada.

Keaton Inkol and John McPhee are with Systems Design Engineering, University of Waterloo, Canada kainkol@uwaterloo.net

978-1-7281-1178-0/21/$31.00 ©2021 IEEE

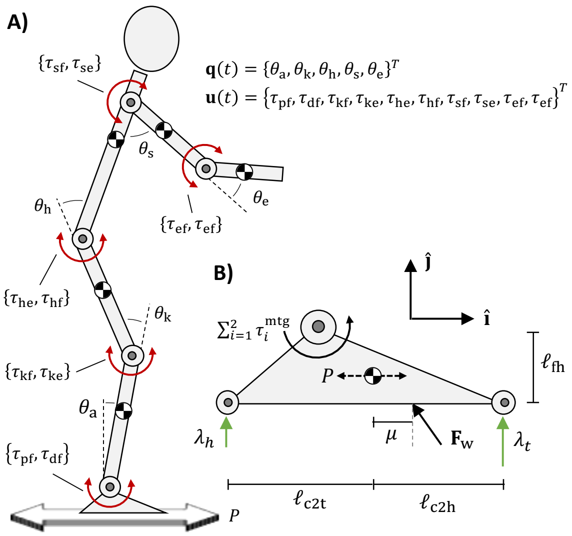

Fig. 1. **A**) Schematic of the planar MTG-driven model; balance recovery was evoked via unexpected accelerations of the support surface (P). **B**) Model of the base of support used to derive the toe/heel constraint forces that dictate postural stability.

and elbow joints were assumed to behave symmetrically; therefore, each pair was represented by a single revolute joint (angles contained in $\mathbf{q}(t)$). The base of support (BOS; combined right/left foot) was rigidly fixed to a motion-driven platform that could be displaced in the anteroposterior direction. This platform was used to deliver balance perturbations to the model [2]. Inertial and geometric parameters for body segments were adopted from the anthropometric tables in [21], [25] (scaled to height = 1.80 m; mass = 75 kg).

Joints were actuated actively and passively using muscle torque generators (MTGs) [15], [18], [19]. Rather than adding biofidelity through redundant muscles, a rotational single muscle-equivalent was implemented for each direction of rotation (flexion, extension). Using torque-scaling functions, MTGs can mimic muscle length/velocity dependencies using the relevant joint angle and velocity. More explicitly, the i^{th} MTG torque that drives the j^{th} joint was given by

$$\tau_i^{\text{mtg}} = u_i(t) \cdot \tau_{\text{pos}}(q_j) \cdot \tau_{\text{vel}}(\dot{q}_j) + \tau_{\text{psv}}(\mathbf{q}, \dot{q}_j) \qquad (1)$$

where u_i is the MTG's isometric activation torque [15] and τ_{pos} and τ_{vel} are scaling functions that depend only on local joint kinematics (equations/parameters for postural MTGs [19]; arm MTGs [17], [18]). Note that in the case of the postural joints (ankle, knee, hip), passive mechanical torques (τ_{psv}) were a function of multiple joint kinematics; an elastic model that considers biarticular muscles was used [16]. The arm $\tau_{\text{psv}}(q_j, \dot{q}_j)$ passive torque and its relevant parameters were adopted from [17]. Joint damping was added to τ_{psv} through a linear rotational damper [20].

B. Nonlinear Model Predictive Control

NMPC was used to generate forward dynamic simulations of humanoid balance recovery. Briefly, NMPC involves solving a nonlinear optimal control problem for a control-oriented model over a future finite horizon $[t_0, t_f]$. The first controller action is then enacted on the system; the process is subsequently repeated at user-defined time steps *ad infinitum*. The finite-horizon optimal control problem takes the form

$$\arg \min_{\mathbf{x}(t),\mathbf{u}(t)} J(\mathbf{x}(t), \mathbf{u}(t)) = \int_{t_0}^{t_f} \mathcal{L}(\mathbf{x}(t), \mathbf{u}(t)) dt \qquad (2)$$

$$\text{subject to: } \dot{\mathbf{x}}(t) = \mathbf{f}(\mathbf{x}(t), \mathbf{u}(t)) \qquad (3)$$

$$\mathbf{H}(\mathbf{x}(t), \mathbf{u}(t); \mathbf{x}(t_0), \mathbf{u}(t_0)) < \mathbf{0} \qquad (4)$$

where $\mathbf{x}(t) = \{\mathbf{q}(t), \dot{\mathbf{q}}(t)\}^T$, $\mathbf{u}(t) \in \mathbb{R}^{10}$ is a vector containing the time-varying isometric activation torques for each MTG (Fig. 1), and $\mathbf{f}$ is the human musculoskeletal control-oriented dynamics that *exclude* any accelerations of the BOS. All linear/nonlinear inequality and box constraints were contained within the vector $\mathbf{H}$. The function $\mathcal{L}$ is typically referred to as the Lagrangian term. As the goal in the current study was to assess how individual criteria influence the observed balance recovery strategies, multi-objective costs were ignored. Rather, the balance responses generated by different Lagrangians were compared. This decision circumvented additional issues like manually tuning weights between performance criteria [8].

The optimal control problem given by (2), (3), (4) was formulated as a nonlinear programming problem (NLP) via direct collocation, i.e. parameterization of state and control trajectories. Trapezoidal collocation was used to ensure (3) could be met with fewer computations. Thus, the control signal sent from the NMPC to the plant was a linear interpolation between the first two controller actions (separated by a step duration) returned by the optimization routine.

C. Cost Function: Lagrangians

1) Joint/State-Space Criteria: The first criteria related to deviations in joint-space was inspired by an optimized pose controller that could respond to multi-directional perturbations [11]. The corresponding Lagrangian minimizes deviations from some reference pose $\bar{\mathbf{q}} = \{\bar{\theta}_a, \bar{\theta}_k, \bar{\theta}_h, \bar{\theta}_s \bar{\theta}_e\}^T$:

$$\Delta\text{Pose: } \mathcal{L}(\cdot) = (\mathbf{q}(t) - \bar{\mathbf{q}})^T (\mathbf{q}(t) - \bar{\mathbf{q}}) \qquad (5)$$

Rather than weigh all elements of $\mathbf{q}$ evenly, individual joints can also be of focus. For example, motion of the knee joint, often imposed as a constraint in models of humanoid stance [7], can be incorporated within the cost functional:

$$\Delta\text{Knee: } \mathcal{L}(\cdot) = (\theta_k - \bar{\theta}_k)^2 \qquad (6)$$

Many simulation studies also have made use of segmental trunk pitch relative to an absolute reference angle $\bar{\theta}_t$ [7], [8]:

$$\Delta\text{Trunk: } \mathcal{L}(\cdot) = (\theta_a + \theta_k + \theta_h - \bar{\theta}_t)^2 \qquad (7)$$

This term assumes head, and subsequently eye position, is regulated by the CNS.

2) Center of Mass Criteria: Criteria related to the control of balance in the whole-body center of mass (COM) space included minimizing horizontal excursions of the COM,

$$\Delta\text{COM: } \mathcal{L}(\cdot) = (\mathbf{r}_{\text{CM}}(\mathbf{q}(t)) \cdot \hat{\mathbf{i}} - \bar{r})^2 \qquad (8)$$

where $\mathbf{r}_{\text{CM}}$ is the COM position. The reference point $\bar{r}$, is the COM position evaluated at $\bar{\mathbf{q}}$. This term can also be expanded to regulate deviations of r_{xCM} which is the COM position extrapolated in the direction of its normalized velocity [23],

$$r_{\text{xCM}} = \{\mathbf{r}_{\text{CM}}(\mathbf{q}(t)) + \sqrt{\frac{\ell_p}{g}}\dot{\mathbf{r}}_{\text{CM}}(\mathbf{x}(t))\} \cdot \hat{\mathbf{i}} \tag{9}$$

$$\Delta\text{XCOM: } \mathcal{L}(\cdot) = (r_{\text{xCM}} - \bar{r})^2 \tag{10}$$

where g is gravitational acceleration and ℓ_p is the theoretical pendulum length for human stance [23]. This term adds a dynamic velocity-component to the performance criteria.

3) Energy/Effort-Based Criteria: Consistent with the human balance recovery literature [7], [8], effort was also considered in the list of performance criteria. In the current study, effort was quantified using squared activation torques,

$$\text{ACT: } \mathcal{L}(\cdot) = \mathbf{u}(t)^T\mathbf{u}(t) \tag{11}$$

Often, these terms promote reasonable movements within dynamic simulations of human motion [22].

D. Domain of Feasibility for Balanced Posture

The domain of feasibility within the NMPC, enforced through Eq. (4), was considered to be the set of all stable motions. For the biped system herein, i.e. foot rigid body is flat against the ground, a state was considered stable so long as the following conditions were met [24]:

$$\begin{Bmatrix} -\mathbf{F}_{\text{w}} \cdot \hat{\mathbf{j}} \\ \mu(\mathbf{x}(t), \mathbf{u}(t)) - \ell_{\text{c2t}} \\ -\ell_{\text{c2h}} - \mu(\mathbf{x}(t), \mathbf{u}(t)) \end{Bmatrix} < \mathbf{0} \tag{12}$$

where $\mathbf{F}_{\text{w}}$ is the contact force between foot and ground, μ is the location of the zero-moment point (ZMP; coincident with the centre of pressure while in the BOS) with respect to the foot COM [24], and ℓ_{c2h},ℓ_{c2t} are the horizontal distance between the foot COM and toe/heel respectively, i.e. the ZMP must remain within BOS boundaries.

For the sake of computational efficiency, the dimension of Eq. (12) was reduced by assuming the foot was hinged to the support surface at two anatomical locations (toes/head of metatarsals and the heel/calcaneus). This approach is similar to previous biomechanical simulations in which heel-raise was permitted using a torsional spring [10]. From the ZMP equations, the following linear system was reached, which assumes that the BOS and inertial frame are parallel:

$$\begin{bmatrix} \ell_{\text{c2t}} & -\ell_{\text{c2h}} \\ 1 & 1 \end{bmatrix} \begin{Bmatrix} \lambda_{\text{t}} \\ \lambda_{\text{h}} \end{Bmatrix} = \begin{Bmatrix} \sum_{i=1}^{n} \tau_{\text{i}}^{\text{mtg}} - \frac{\ell_{\text{fh}}}{2}\mathbf{F}_{\text{w}} \cdot \hat{\mathbf{i}} \\ \mathbf{F}_{\text{w}} \cdot \hat{\mathbf{j}} \end{Bmatrix} \tag{13}$$

The normal contact forces acting at the toe (λ_{t}) and heel (λ_{h}), were then used in (4): $H_1 = -\lambda_{\text{t}}$ and $H_2 = -\lambda_{\text{h}}$. One of these forces becoming negative would indicate rotation of the foot about the opposing marker; both would indicate that the model has become fully airborne.

For an infinite horizon, Eq. (12) alone would be sufficient in guaranteeing stability in the NMPC. However, for receding horizon control, this is often not the case. To improve stability without expanding the number of terms in (2), a relaxed terminal constraint was added to $\mathbf{H}$. The horizontal XCOM and vertical COM positions at t_f were constrained to remain within the confines of a small ellipse centered at the reference pose COM position $(\bar{r}, \bar{h})$:

$$H_3 = \frac{(r_{\text{xCM}}(\mathbf{x}(t_f)) - \bar{r})^2}{s_x^2} + \frac{(\mathbf{r}_{\text{CM}}(\mathbf{q}(t_f)) \cdot \hat{\mathbf{j}} - \bar{h})^2}{s_y^2} - 1 \tag{14}$$

Here, s_x and s_y are the horizontal and vertical semiaxes. Constraining COM height encourages a return towards upright posture, whereas doing the same for the XCOM can leave the humanoid in a posture that is theoretically recoverable (assuming the body behaves like an inverted pendulum [23]). Similar criteria have appeared as Mayer terms in previous dynamic simulations of balance recovery [8], [10].

E. Simulation Experiments

A series of simulation experiments were conducted to mimic an existing and well-known experimental protocol [2], in which healthy young adults were subjected to support-surface translations in four directions. Perturbations were based on a piecewise acceleration function consisting of a propulsive and braking impulse; the function parameters were tuned according to the differences in recovery difficulty between directions, i.e. the probability of inducing a change in support. In the current study, "small" forward and backward perturbations were selected [2], which in experiments triggers balance recovery with a low likelihood of stepping. Simulations, spanning a two-second window [8], were then run for each combination of Lagrangian (see II-C), perturbation direction (backward and forward), and upper limb condition (arms locked, AL; arms free, AF). Accelerations of the support surface were initiated 150 ms after the beginning of each simulation.

The optimal control problem embedded within the NMPC controller was scaled and solved using an interior-point method in `fmincon` (MATLAB 2020a, MathWorks, USA). Symbolic gradients and Hessians were generated in MapleSim, exported into optimized MATLAB/C++ functions, and supplied to the solver to improve controller efficacy. Controller step size and horizon length were set to 25 ms and 800 ms respectively; additional parameters included $\bar{\mathbf{q}} = \{-4.6, 2.9, -2.9, 0, 0\}^T$ deg and $s_x = s_y = 2.5$ cm. Parameter values were based on the limited literature in modelling human motor control via MPC [4], [5].

Given our interest in the functionality of simulated arm responses, a quantitative measure was introduced to assess whether unlocking the arm joints would improve the performance under each criteria. This measure, the logarithmic cost ratio (CR), was evaluated as, CR $= \log_{10}(J_{\text{AF}}/J_{\text{AL}})$ which effectively indicated whether the arms reduced the given cost of recovery (CR<0) while also accounting for the varying orders of magnitude between evaluated functionals.

III. RESULTS AND DISCUSSION

The postural strategies generated using each performance criteria are shown in Fig. 2. Some notable features within the results of the AL condition include the following: When using ΔPose, NMPC relied on a general stiffening strategy to minimize all joint deviations for both perturbation directions.

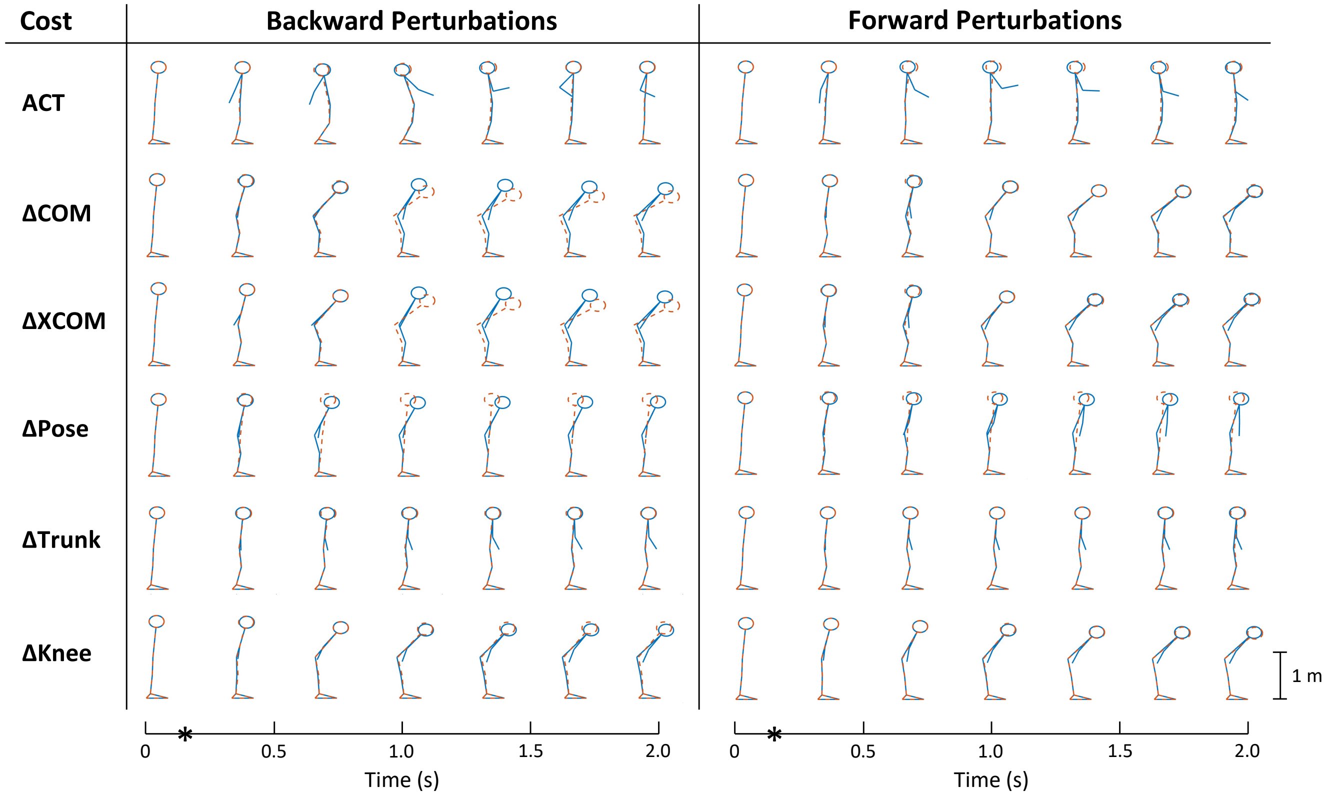

Fig. 2. Simulated postural responses following backward (*left*, initial fall forward) and forward (*right*, initial fall backward) support-surface perturbations with the arm joints locked (*dotted figure*) or free (*solid figure*). Responses were generated using the six optimality criteria shown. Peturbation initiation is marked by * on the time axis.

The ΔKnee criteria forced the biomechanical model to adopt a classic double pendulum (combined hip-ankle) strategy [3], [7]. Using ΔCOM and ΔXCOM produced near-identical multi-joint COM lowering strategies with some minor perturbation direction-dependencies, e.g. patterns of ankle and hip sway. Unsurprisingly, the ACT criteria prompted the model to relax the most during the recovery, especially for the backward condition. Versteeg et al. [8] reported that increasing the relative weights on muscle stress criteria in dynamic musculoskeletal simulations prompted a shift towards a hip strategy following backward perturbations. In the current study, without additional regulatory criteria [8], the NMPC became reliant on passive MTG terms and moved the model through awkward poses rather than using a defined hip strategy. Formulations using net joint torques may produce more reasonable behaviours as factors like parallel elastic tension and injury limits are considered.

Following a forward perturbation, both ACT and ΔTrunk criteria produced peak backward XCOM excursions relative to the heel (-5.0 to -1.7 cm) that were similar to experimental values using the same perturbation (-4.8 cm [28]). Conversely, XCOM excursions following backward perturbations were consistently underestimated using NMPC, though variables like peak forward trunk pitch did match those in the literature (e.g. -50 to -40° [8]) despite differences in perturbation size. These predictions were best when using ΔCOM or ΔXCOM; ΔKnee provided a markedly close match also (-38.2° with AL). It is likely that using a weighted combination of multiple criteria (e.g. ACT + ΔCOM) would correct these reported prediction errors [7], [8], [22].

TABLE I
Evaluated Logarithmic Cost Ratios (CR)

	Joint-Space			COM-Space		Effort
Dir.	ΔPose	ΔKnee	ΔTrunk	ΔCOM	ΔXCOM	ACT
B	2.13	**-2.61**	**-2.54**	**-1.14**	**-0.82**	**-0.05**
F	2.38	**-0.61**	0.99	0.46	0.04	0.05

Unlocking the arm joints had a handful of interesting effects on the simulated postural kinematics (Fig. 2). Most notably, the ΔPose-predicted balance strategy shifted from stiffening to using pronounced flexion of the knee and hip (occurred for both perturbation directions). Additionally, having the arms locked appeared to make it easier for the NMPC to minimize knee or trunk deviations, as reflected by the CRs in Table I. Most of the observed effects took place in the backward perturbation condition (Table I). For example, unlocking the arms while using ΔCOM and ΔXCOM modified the predicted ankle/hip trajectories in said condition only; no obvious changes exist for the forward condition. In general, unlocking the arms had less of an impact on the forward perturbation responses than anticipated [13], [26].

The compensatory arm responses generated for each combination of Lagrangian and perturbation direction are also summarized in Fig. 2. Extremely similar patterns were observed for ΔKnee, ΔTrunk, ΔCOM, ΔXCOM: a slow drift towards flexion in shoulder and elbow following each perturbation. This lack of sizable arm motion could be due to numerous factors, e.g. less arm movement is optimal, local NLP methods and restrictive initial guess not capturing global optimum, too small a perturbation, and the need for a 3D model to capture phenomena [13], [26]. Unfortunately, cases like ΔKnee, where the CR<0 but there is no unique arm response, make it difficult to assess whether CR improvements were purely coincidental. The exaggerated arm responses observed when using the ACT criteria is consistent with the corresponding lower-limb responses; an oscillatory behaviour is particularly noticeable in the shoulder. Interestingly, ΔPose had unique arm motions paired with the corresponding *flexed* postural strategy, particularly following forward perturbations. The shoulders were slowly flexed forward and the elbow was maintained nearly straight, i.e. counterbalancing. However, the CR for ΔPose was positive, which suggests that the different control strategy emerged as a byproduct of the relative location of the initial guess within the AF and AL search spaces.

IV. Conclusion

In summary, few cost functions within the NMPC scheme, e.g. ΔPose and ACT, generated substantial compensatory arm movements in a planar biomechanical model of human balance recovery. There are various assumptions, limitations and potential future directions for the current study. Neural delays, notably during 80-100 ms following the perturbation [3], [8], weren't considered to keep the current NMPC iteration simple; future iterations will add delays to improve fidelity. Friction was not considered within the domain of feasibility for balanced posture; though during simulations, the tangential ground reaction force never exceeded a reasonable dry friction threshold (coefficient = 0.20, [25]). It was assumed within the NMPC that the CNS formulates the control problem primarily through Lagrangian terms. The addition of Mayer terms to the embedded problem, as well as any Lagrangian criteria not examined herein, would require further research. Additionally, given the infrequent use of MPC in biomechanical predictive simulations, further system identification may be beneficial in providing direction to biomechanics researchers during MPC design [5], [4]. It is possible that this process would naturally require establishment of the proper optimal control problem formulation.

References

[1] T. M. Morrison, P. Pathmanathan, M. Adwan, and E. Margerrison, "Advancing Regulatory Science With Computational Modeling for Medical Devices at the FDA's Office of Science and Engineering Laboratories," Front. Med., vol. 5, pp. 241, 2018.

[2] B. E. Maki, W. E. McIlroy, and S. D. Perry, "Influence of lateral destabilization on compensatory stepping responses," J Biomech, vol. 29, pp. 343–353, 1996.

[3] F. B. Horak and L. M. Nashner, "Central programming of postural movements: adaptation to altered support-surface configurations," J Neurophysiol, vol. 5, pp. 1369–1381, 1986.

[4] Z. Aftab, T. Robert, and P.-B. Wieber, "Balance Recovery Prediction with Multiple Strategies for Standing Humans", PLOS ONE, vol. 11, pp. e0151166, 2016.

[5] N. Mehrabi, R. Sharif Razavian, B. Ghannadi, and J. McPhee, "Predictive Simulation of Reaching Moving Targets Using Nonlinear Model Predictive Control," Front Comput Neurosc, vol. 10, pp. 143, 2017.

[6] K.A. Inkol and J. McPhee. "Assessing Control of Fixed-Support Balance Recovery in Wearable Lower-Limb Exoskeletons Using Multibody Dynamic Modelling," 8th IEEE RAS/EMBS Int Conf Biomed Rob & Biomech (BioRob), pp. 54–60, 2020.

[7] A. D. Kuo, "An optimal control model for analyzing human postural balance," IEEE T Bio-Med Eng, vol. 42, pp. 87–101, 1995.

[8] C. S. Versteeg, L. H. Ting, and J. L. Allen, "Hip and ankle responses for reactive balance emerge from varying priorities to reduce effort and kinematic excursion: A simulation study," J Biomech, vol. 49, pp. 3230–3237, 2016.

[9] F. De Groote, J. L. Allen, and L. H. Ting, "Contribution of muscle short-range stiffness to initial changes in joint kinetics and kinematics during perturbations to standing balance: A simulation study," J Biomech, vol. 55, pp. 71–77, 2017.

[10] K. B. Cheng, H. Tanabe, W.-C. Chen, and H.-T. Chiu, "Role of heel lifting in standing balance recovery: A simulation study," J Biomech, vol. 67, pp. 69–77, 2018.

[11] K. Kaminishi, P. Jiang, R. Chiba, K. Takakusaki, and J. Ota, "Postural control of a musculoskeletal model against multidirectional support surface translations," PLOS ONE, vol. 14, pp. e0212613, 2019.

[12] M. Mansouri, A. E. Clark, A. Seth, and J. A. Reinbolt, "Rectus femoris transfer surgery affects balance recovery in children with cerebral palsy: A simulation study," Gait Posture, vol. 43, pp. 24–30, 2016.

[13] K. A. Inkol, A. H. Huntley, and L. A. Vallis, "Repeated Exposure to Forward Support-Surface Perturbation During Overground Walking Alters Upper-Body Kinematics and Step Parameters," J Motor Behav, vol. 51, pp. 318-330, 2018.

[14] M. Nakada, B. Allen, S. Morishima, and D. Terzopoulos, "Learning Arm Motion Strategies for Balance Recovery of Humanoid Robots," Int Conf Emerging Secur Technol, Canterbury, UK, pp.165–170, 2010.

[15] K. A. Inkol, C. Brown, W. McNally, C. Jansen, and J. McPhee, "Muscle torque generators in multibody dynamic simulations of optimal sports performance," Multibody Syst Dyn, vol. 50, pp. 435-452 2020.

[16] R. Riener and T. Edrich, "Identification of passive elastic joint moments in the lower extremities," J Biomech, vol. 32, pp. 539–544,1999.

[17] C. Brown and J. McPhee, "Predictive Forward Dynamic Simulation of Manual Wheelchair Propulsion on a Rolling Dynamometer," J Biomech Eng, vol. 142, pp. 071008, 2020.

[18] M. R. Yeadon, M. A. King, and C. Wilson, "Modelling the maximum voluntary joint torque/angular velocity relationship in human movement," J Biomech, vol. 39, pp. 476–482, 2006.

[19] D. E. Anderson, M. L. Madigan, and M. A. Nussbaum, "Maximum voluntary joint torque as a function of joint angle and angular velocity: model development and application to the lower limb," J Biomech, vol. 40, pp. 3105–3113, 2007.

[20] G. T. Yamaguchi, Dynamic modeling of musculoskeletal motion: a vectorized approach for biomechanical analysis in three dimensions, New York, NY: Springer, 2006.

[21] D. A. Winter, Biomechanics and motor control of human movement, 4th ed. Hoboken, N.J: Wiley, 2009.

[22] D. Clever, R. Malin Schemschat, M. L. Felis, and K. Mombaur, "Inverse optimal control based identification of optimality criteria in whole-body human walking on level ground," 6th IEEE Int Conf Biomed Rob & Biomech (BioRob), Singapore, pp. 1192–1199, 2016.

[23] A. L. Hof, M. G. J. Gazendam, and W. E. Sinke, "The condition for dynamic stability," J Biomech, vol. 38, pp. 1–8, 2005.

[24] M. Vukobratović and B. Borovac, "Zero-Moment Point — Thirty Five Years of its Life," Int J Human Robot, vol. 1, pp. 157–173, 2004.

[25] Y. C. Pai and J. Patton, "Center of Mass Velocity-Posiion Predictions For Balance Control" J Biomech, vol. 30, pp. 347–354, 1997.

[26] P. Corbeil, B. R. Bloem, M. van Meel, and B. E. Maki, "Arm reactions evoked by the initial exposure to a small balance perturbation: A pilot study," Gait Posture, vol. 37, pp. 300–303, 2013.

[27] K. L. Troy, S. J. Donovan, and M. D. Grabiner, "Theoretical contribution of the upper extremities to reducing trunk extension following a laboratory-induced slip," J Biomech, vol. 42, pp. 1339–1344, 2009.

[28] K. A. Inkol and L. Vallis, "Modelling the dynamic margins of stability for use in evaluations of balance following a support-surface perturbation," J Biomech, vol. 95, pp. 109302, 2019.